Available online at www.sciencedirect.com
SCIENCE DIRECT®
International Journal of Thermal Sciences 45 (2006) 923–931
International Journal of Thermal Sciences
www.elsevier.com/locate/ijts

Free convection heat transfer from a horizontal cylinder affected by a downstream parallel cylinder of different diameter

Claudio Cianfrini, Massimo Corcione *, Emanuele Habib

Dipartimento di Fisica Tecnica, University of Rome "La Sapienza", via Eudossiana, 18-00184 Rome, Italy

Received 2 August 2005; received in revised form 30 September 2005; accepted 4 November 2005

Available online 19 January 2006

Abstract

Steady laminar free convection in air from an isothermal horizontal cylinder affected by a superimposed parallel cylinder of different diameter, either at same temperature of the underneath cylinder or adiabatic, is studied numerically. A specifically developed computer-code based on the SIMPLE-C algorithm is used for the solution of the mass, momentum, and energy governing equations. Simulations are performed for ratios between the diameters of the upper and lower cylinders from 0 to 125, for inter-cylinder spacings from 0.1 up to more than 20 diameters of the bottom cylinder, and for values of the Rayleigh number in the range between 10^1 and 10^7. It is found that (a) for cylinder-spacings smaller than a first critical distance, the heat transfer performance of the bottom cylinder degrades owing to the presence of the top cylinder, whichever is the temperature condition imposed at the top cylinder surface, and (b) the thermal state of the upper cylinder surface starts being effective on the thermal behavior of the bottom cylinder once the cylinder-spacing is further reduced below a second critical distance. Dimensionless correlating-equations for the calculation of the heat transfer rate at the bottom cylinder surface, and of the first and second critical distances cited above, are also proposed.

Keywords: Laminar free convection; Horizontal cylinders; Vertical confinement; Correlating equations; Numerical analysis

1. Introduction

Free convection heat transfer from an isothermal horizontal cylinder suspended in an infinite medium has been extensively investigated analytically, numerically, and experimentally [1–14]. Indeed, in many technological applications, the fluid medium around the cylinder is partially or completely confined, which may imply dramatic changes in the amount of heat and momentum transferred. Nonetheless, published works readily available in the open literature are relatively few, and mainly deal with the horizontal confinement [15–22].

As regards the vertical confinement above the cylinder, which the present work addresses, Koizumi and Hosokawa [23] conducted experiments aimed to reveal the effects produced by a flat ceiling on the flow and heat transfer performance around a heated horizontal cylinder suspended in air, for Rayleigh numbers ranging from 4.8×10^4 to 10^7. The authors showed the existence of three types of flow patterns depending on the Rayleigh number, the distance between the ceiling and the cylinder, and the temperature condition of the ceiling for a variety of flow situations. Successively, Atmane et al. [24] investigated the dynamics of the plume above a heated horizontal cylinder mounted in a water tank and vertically confined by the water free surface, for Rayleigh numbers in the range between 10^6 and 10^7. They found that, for depths of the cylinder below the free surface up to three cylinder-diameters, the primary effect of the vertical confinement are increases in heat flux at the top of the cylinder. For water levels larger than three diameters, no significant difference in the thermal behavior of the cylinder with respect to the case of unconfined fluid medium was observed.

In contrast to both papers mentioned above, in which the fluid medium around the hot cylinder is confined by either a cold or an adiabatic flat surface larger than the cylinder-diameter, the case of vertical confinement obtained through a curved body of finite size at same temperature of the underneath

* Corresponding author.
E-mail address: massimo.corcione@uniroma1.it (M. Corcione).

1290-0729/$ – see front matter
doi:10.1016/j.ijthermalsci.2005.11.008

Nomenclature

d	bottom cylinder diameter	m	
D	top cylinder diameter	m	
$\mathbf{g}$	gravity vector	$m\,s^{-2}$	
g	gravitational acceleration	$m\,s^{-2}$	
h	average coefficient of convection heat transfer	$W\,m^{-2}\,K^{-1}$	
$h(\theta)$	local coefficient of convection heat transfer	$W\,m^{-2}\,K^{-1}$	
k	thermal conductivity of the fluid	$W\,m^{-1}\,K^{-1}$	
Nu_b	average Nusselt number of the bottom cylinder, $= hd/k$		
Nu_0	average Nusselt number of the single cylinder, $= hd/k$		
$Nu(\theta)$	local Nusselt number, $= h(\theta)d/k$		
p	dimensionless pressure		
Pr	Prandtl number, $= \nu/\alpha$		
Q	heat transfer rate	W	
q	heat flux	$W\,m^{-2}$	
r	dimensionless radial coordinate		
Ra	Rayleigh number, $= g\beta(t_w - t_\infty)d^3/\alpha\nu$		
S	inter-cylinder spacing	m	
T	dimensionless temperature		
t	temperature	K	
U	dimensionless vertical or radial velocity component		
$\mathbf{V}$	dimensionless velocity vector		
V	dimensionless horizontal or tangential velocity component		
X	dimensionless vertical coordinate		
Y	dimensionless horizontal coordinate		

Greek symbols

α	thermal diffusivity of the fluid	$m^2\,s^{-1}$
β	coefficient of thermal expansion of the fluid	K^{-1}
ν	kinematic viscosity of the fluid	$m^2\,s^{-1}$
θ	dimensionless polar coordinate	
ρ	density of the fluid	$kg\,m^{-3}$

Subscripts

w	referred to the cylinder surface
∞	referred to the undisturbed fluid reservoir

cylinder has been much less studied. In fact, despite several studies on natural convection from vertical arrays of isothermal horizontal cylinders set in free space have been performed, most of them were carried out for large spacings [25–29]. The only exception is the experimental study conducted by Tokura et al. [30], in which decreases in heat flux at the upper part of the bottom cylinder of the array were detected for the smallest inter-cylinder spacing investigated.

In this background, the aim of the present paper is to carry out a numerical analysis of free convection in air from an isothermal horizontal cylinder affected by a superimposed parallel cylinder of different diameter, either at same temperature of the underneath cylinder or adiabatic. The study is performed under the assumption of a two-dimensional steady laminar flow, for ratios between the diameters of the upper and lower cylinders from 0 to 125, for inter-cylinder spacings from 0.1 up to more than 20 diameters of the bottom cylinder, and for values of the Rayleigh number based on the diameter of the bottom cylinder in the range between 10^1 and 10^7.

2. Mathematical formulation

The geometrical configuration consisting of two superimposed horizontal circular cylinders shown in Fig. 1 is considered. Free convection heat transfer occurs between the bottom cylinder surface, kept at a uniform temperature t_w, and the surrounding undisturbed fluid reservoir, assumed at a uniform temperature t_∞. For the top cylinder, both conditions of uniform temperature t_w and of adiabatic boundary surface, are considered.

The buoyancy-induced flow is considered to be steady, two-dimensional, and laminar. The fluid is assumed to be incompressible, with constant physical properties and negligible viscous dissipation and pressure work. The buoyancy effects on momentum transfer are taken into account through the Boussinesq approximation.

Once the above assumptions are employed in the conservation equations of mass, momentum, and energy, the following set of dimensionless governing equations is obtained:

$$\nabla \cdot \mathbf{V} = 0 \tag{1}$$

$$(\mathbf{V} \cdot \nabla)\mathbf{V} = -\nabla p + \nabla^2 \mathbf{V} - \frac{Ra}{Pr} T \frac{\mathbf{g}}{g} \tag{2}$$

$$(\mathbf{V} \cdot \nabla)T = \frac{1}{Pr} \nabla^2 T \tag{3}$$

where $\mathbf{V}$ is the velocity vector having dimensionless velocity components U and V normalized with ν/d; T is the dimensionless temperature excess over the uniform temperature of the surrounding undisturbed fluid normalized with the temperature difference $(t_w - t_\infty)$; and p is the dimensionless pressure normalized with $\rho_\infty \nu^2/d^2$.

The related boundary conditions are: (a) $\mathbf{V} = 0$ and $T = 1$ at the bottom cylinder surface; (b) $\mathbf{V} = 0$ and $\partial T/\partial r = 0$ or $T = 1$ at the top cylinder surface, depending on whether the top cylinder surface is adiabatic or maintained at the same temperature of the bottom cylinder surface; and (c) $\mathbf{V} = 0$ and $T = 0$ at very large distance from both cylinders.

3. Discretization grid system

The finite-difference solution of the governing equations (1)–(3) with the boundary conditions stated above requires that a discretization grid system is established across the whole integration domain. Since the flow is symmetric about the vertical

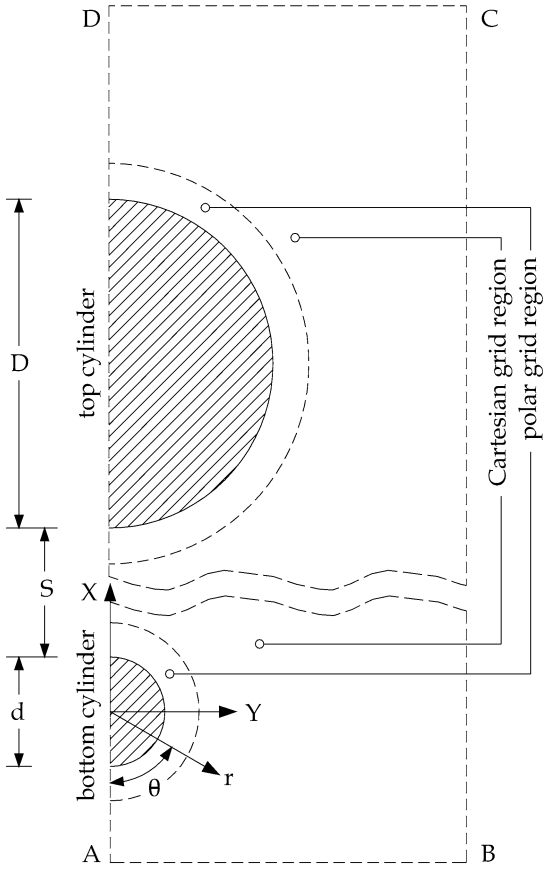

Fig. 1. Schematic of the geometry and coordinate systems.

plane passing through the axes of both cylinders, the 2D integration domain is assumed to extend from the vertical symmetry line and the two half-cylinder surfaces up to a rectangular pseudo-boundary line set sufficiently far away from both cylinders.

As far as the discretization of such domain is concerned, a cylindrical polar grid is employed in the proximity of each cylinder, whilst a Cartesian grid is used to fill the remainder of the integration domain, as shown in Fig. 1. The r and θ coordinates of the polar systems are measured from the center of the cylinders, and anti-clockwise from the downward vertical line, respectively. In both polar systems, U is the radial velocity component, and V is the tangential velocity component. As regards the Cartesian system, whose origin is taken at the center of the bottom cylinder, the X-axis is vertical and pointing upwards in the direction opposite to the gravity vector, whilst the Y-axis is horizontal. In this system, U is the vertical velocity component, and V is the horizontal velocity component.

According to the discretization scheme originally developed by Launder and Massey [31], the cylindrical polar grids and the Cartesian grid, which are entirely independent of one another, overlap with no attempt of node-matching. Their connection is provided by a row of false nodes, one for each neighboring grid, located beyond their intersection. Additional details on the matching regions can be found in references [29,31].

4. Boundary conditions

The boundary conditions required for the numerical solution of the governing equations (1)–(3) have to be specified at each of the boundary lines which enclose the two-dimensional integration domain defined above. As far as the rectangular pseudo-boundary line is concerned, once this is placed sufficiently far away from the cylinders, the fluid may be reasonably assumed to enter or leave the integration flow-domain in the direction normal to the boundary line. The entering fluid is assumed at the ambient temperature. As regards the leaving fluid, whose temperature is not known *a priori*, a zero temperature gradient normal to the boundary line is assumed, thus implying that the local heat transfer is dominated by convection rather than by conduction, provided that the outflow velocity is sufficiently large.

Thus, the following boundary conditions are applied:

(a) at the left symmetry line A–D

$$\frac{\partial U}{\partial Y}=0, \qquad V=0, \qquad \frac{\partial T}{\partial Y}=0 \tag{4}$$

(b) at the bottom half-cylinder surface

$$U=0, \qquad V=0, \qquad T=1 \tag{5}$$

(c) at the top half-cylinder surface

$$U=0, \qquad V=0, \qquad T=1 \quad \text{or} \quad \frac{\partial T}{\partial r}=0 \tag{6}$$

(d) at the bottom boundary line A−B

$$\frac{\partial U}{\partial X}=0, \qquad V=0$$
$$T=0 \quad \text{if } U\geqslant 0 \quad \text{or} \quad \frac{\partial T}{\partial X}=0 \quad \text{if } U<0 \tag{7}$$

(e) at the right boundary line B–C

$$U=0, \qquad \frac{\partial V}{\partial Y}=0$$
$$T=0 \quad \text{if } V<0 \quad \text{or} \quad \frac{\partial T}{\partial Y}=0 \quad \text{if } V\geqslant 0 \tag{8}$$

(f) at the top boundary line C–D

$$\frac{\partial U}{\partial X}=0, \qquad V=0$$
$$T=0 \quad \text{if } U<0 \quad \text{or} \quad \frac{\partial T}{\partial X}=0 \quad \text{if } U\geqslant 0 \tag{9}$$

Moreover, as far as the intersections between polar and Cartesian grids are concerned, the value of each of the dependent variables at any false node of one of the two neighboring grids is obtained by a linear interpolation of the values of the same variable at the four surrounding real nodes of the other grid.

5. Solution procedure

The set of governing equations (1)–(3) with the boundary conditions (4)–(9) is solved through a control-volume formulation of the finite-difference method. The pressure–velocity coupling is handled by the SIMPLE-C algorithm by Van Doormaal

Table 1
Comparison of the present results with the benchmark solutions of Saitoh et al. [12] and other results

Ra		*Nu*(θ)							*Nu*
		θ = 0°	30°	60°	90°	120°	150°	180°	
10^3	Present	3.789	3.755	3.640	3.376	2.841	1.958	1.210	3.023
	Saitoh et al.	3.813	3.772	3.640	3.374	2.866	1.975	1.218	3.024
	Wang et al.	3.860	3.820	3.700	3.450	2.930	1.980	1.200	3.060
	Kuehn and Goldstein	3.890	3.850	3.720	3.450	2.930	2.010	1.220	3.090
10^4	Present	5.986	5.931	5.756	5.406	4.716	3.293	1.532	4.819
	Saitoh et al.	5.995	5.935	5.750	5.410	4.764	3.308	1.534	4.826
	Wang et al.	6.030	5.980	5.800	5.560	4.870	3.320	1.500	4.860
	Kuehn and Goldstein	6.240	6.190	6.010	5.640	4.820	3.140	1.460	4.940
10^5	Present	9.694	9.595	9.297	8.749	7.871	5.848	1.989	7.886
	Saitoh et al.	9.675	9.577	9.278	8.765	7.946	5.891	1.987	7.898
	Wang et al.	9.800	9.690	9.480	8.900	8.000	5.800	1.940	7.970
	Kuehn and Goldstein	10.150	10.030	9.650	9.020	7.910	5.290	1.720	8.000

and Raithby [32], which is essentially a more implicit variant of the SIMPLE algorithm by Patankar and Spalding [33]. The fluxes across the surfaces of the control volumes are evaluated by the QUICK discretization scheme by Leonard [34]. Details on the SIMPLE procedure may be found in Patankar [35].

Fine uniform mesh-spacings are used for the discretization of both the polar grid regions and the Cartesian grid region. Starting from first-approximation distributions of the dependent variables across the integration domain, the discretized governing equations are solved iteratively through a line-by-line application of the Thomas algorithm. Under-relaxation is used to ensure the convergence of the iterative procedure. The solution is considered to be fully converged when the maximum absolute values of both the mass source and the percent changes of the dependent variables at any grid-node from iteration to iteration are smaller than prescribed values, i.e., 10^{-4} and 10^{-6}, respectively.

After convergence is attained, the local and average Nusselt numbers $Nu_b(\theta)$ and Nu_b of the bottom cylinder are calculated:

$$Nu_b(\theta) = \frac{qd}{k(t_w - t_\infty)} = -\frac{\partial T}{\partial r}\bigg|_{r=0.5} \tag{10}$$

$$Nu_b = \frac{Q}{\pi k(t_w - t_\infty)} = -\frac{1}{\pi}\int_0^\pi \frac{\partial T}{\partial r}\bigg|_{r=0.5} \mathrm{d}\theta \tag{11}$$

The temperature gradients at the cylinder surface are evaluated by assuming a second-order temperature profile among each wall-node and the next two fluid-nodes. The integral is approximated by the trapezoid rule.

Tests on the dependence of the results obtained on the mesh-spacing of both the polar and the Cartesian discretization grids, as well as on the thickness of the polar grid regions, and on the extent of the whole computational domain, have been performed for a wide variety of geometrical configurations analyzed and of Rayleigh numbers investigated, in both cases of heated and adiabatic top cylinder. In particular, the optimal grid-size values, and the optimal positions of the polar/Cartesian interface and of the outer pseudo-boundary line, i.e., those used for computations, which represent a good compromise between solution accuracy and computational time required, are assumed as those over which further grid refinements or further boundary displacements do not produce noticeable modifications both in the heat transfer rates and in the predicted flow field. Namely, when the percent changes of the local and average Nusselt numbers defined above, as well as the percent change of the maximum value of the tangential velocity components at $\theta = 90°$ for both cylinders are smaller than prescribed accuracy values, i.e., 1% and 2%, respectively. Typical numbers of nodal points ($r \times \theta$) of the polar discretization grids lie in the range between 45×72 and 270×180, whilst the extent of the whole integration flow-domain ranges between 2 and 20 times the largest of the two cylinder-diameters, depending on the Rayleigh number *Ra*, on the diameter ratio D/d, and on the dimensionless inter-cylinder spacing S/d.

Table 2
Comparison of the present solutions with experimental and numerical results and correlating equations found in literature

Ra	Present	[A]	[B]	[C]	[D]	[E]	[F]	[G]	[H]
10^1	1.421	1.057	1.49	1.49	–	–	1.4	–	1.31
10^2	1.961	1.599	2.10	2.11	–	–	2.05	2.07	2.02
10^3	3.023	2.563	3.14	3.14	3.024	3.06	3.09	3.04	3.11
10^4	4.819	4.278	4.97	4.92	4.826	4.86	4.94	4.85	4.80
10^5	7.886	7.327	8.33	8.05	7.898	7.97	8	8.03	8.54
10^6	13.95	12.75	14.71	13.62	–	13.46	13.52	13.65	15.18
10^7	23.48	22.39	27.28	24.04	–	23.29	23.32	24.00	26.99

[A] Churchill & Chu eqn. [36].
[B] Raithby & Hollands eqn. [37].
[C] Kuehn & Goldstein eqn. [38].
[D] Saitoh et al. num. data [12].
[E] Wang et al. num. data [11].
[F] Kuehn & Goldstein num. data [7].
[G] Clemes et al. exp. data interpolated [13].
[H] Morgan eqns. [4].

Furthermore, in order to validate the numerical code and the composite-grid discretization scheme used in the present study, both the local and the average Nusselt numbers obtained at different Rayleigh numbers for a single cylinder set in free air have been compared with the benchmark numerical data by Saitoh et al. [12] and other results available in the literature [4,7,11–13, 36–38], as shown in Tables 1 and 2, respectively.

An overall good agreement between the present data and published results is noticed. In particular, the present local

Table 3
Comparison of the present solutions for two superimposed horizontal cylinders of the same diameter with experimental data form Tokura et al. [30] and from Sparrow and Niethammer [39]

			Nu/Nu_0 (S/d)			
			0.1	0.3	0.5	1
$Gr = 1.2 \times 10^5$	Bottom cylinder	Present	0.908	–	0.996	1.008
		Tokura et al.	0.89	–	1.00	1.01
	Upper cylinder	Present	0.614	0.661	0.726	0.853
		Tokura et al.	0.61	0.68	0.74	0.87
	Whole array	Present	0.761	0.813	0.861	0.930
		Tokura et al.	0.75	0.81	0.87	0.92
$Ra = 2 \times 10^4$	Upper cylinder	Present	–	–	–	0.810
		Sparrow and Niethammer	–	–	–	0.82
$Ra = 6 \times 10^4$	Upper cylinder	Present	–	–	–	0.844
		Sparrow and Niethammer	–	–	–	0.85
$Ra = 1 \times 10^5$	Upper cylinder	Present	–	–	–	0.856
		Sparrow and Niethammer	–	–	–	0.86

and average heat transfer results are well within $\pm 1\%$ of the benchmark data by Saitoh et al. The only exceptions are represented by the under-predictions of the Churchill–Chu equation in the whole range of the Rayleigh number, and by the over-predictions of the Morgan equations at the largest Rayleigh numbers investigated. In the case of the Churchill–Chu equation, this was expected as in the range $10^1 \leqslant Ra \leqslant 10^7$ such equation falls below the data upon which it was based. In the case of the Morgan equations, this may be explained by considering that Morgan included also data on liquids, yet, in his correlations he did not consider the effects of the Prandtl number.

Additional comparisons between the computed distributions of the dimensionless temperature, radial velocity, and tangential velocity versus the dimensionless radial distance from the cylinder surface at different angles, and the numerical solutions of Saitoh et al. [12], Kuehn and Goldstein [7], and Wang et al. [11] at $Ra = 10^5$ can be found in reference [29].

As far as the present geometrical configuration is specifically concerned, a good agreement has been found with some of the data available in the literature, as shown in Table 3, where the present numerical data are compared with the experimental data obtained by Tokura et al. [30] and by Sparrow and Niethammer [39] at close spacings.

6. Results and discussion

Numerical simulations are performed for $Pr = 0.71$, which corresponds to air, and, in both cases of heated and adiabatic upper cylinder, for different values of (a) the Rayleigh number Ra based on the diameter d of the bottom cylinder in the range between 10^1 and 10^7, (b) the diameter ratio D/d in the range between 0 and 125, and (c) the dimensionless inter-cylinder spacing S/d in the range between 0.1 and more than 20.

6.1. Heat transfer characteristics

The effects of the independent variables Ra, D/d, and S/d on the heat transfer rate at the bottom cylinder surface are shown in Figs. 2 and 3, for both cases of heated and adiabatic upper cylinder. The ordinate of each diagram is the ratio Nu_b/Nu_0 between the average Nusselt numbers for the bottom cylinder and for the single cylinder at same Rayleigh number,

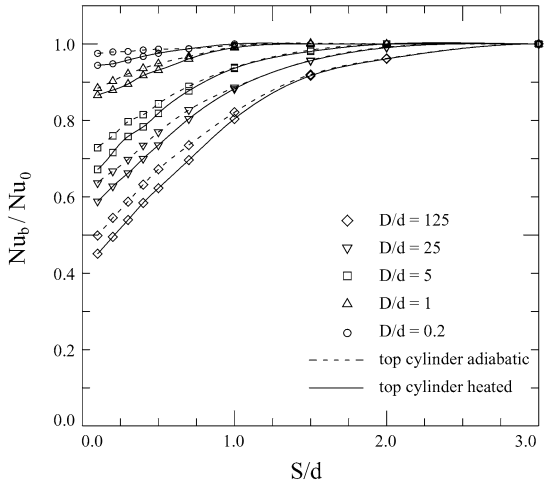

Fig. 2. Distributions of the ratio Nu_b/Nu_0 vs. S/d at $Ra = 10^3$.

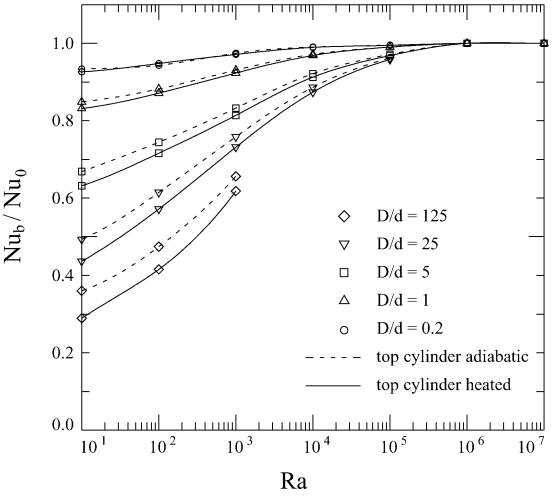

Fig. 3. Distributions of the ratio Nu_b/Nu_0 vs. Ra at $S/d = 0.5$.

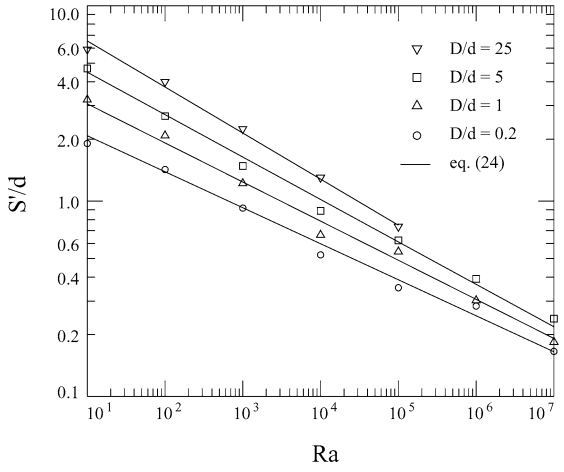

Fig. 4. Distribution of the first critical cylinder-spacing S'/d vs. Ra.

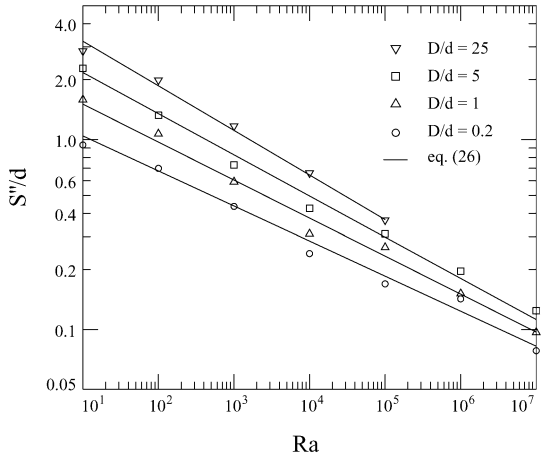

Fig. 5. Distribution of the second critical cylinder-spacing S''/d vs. Ra.

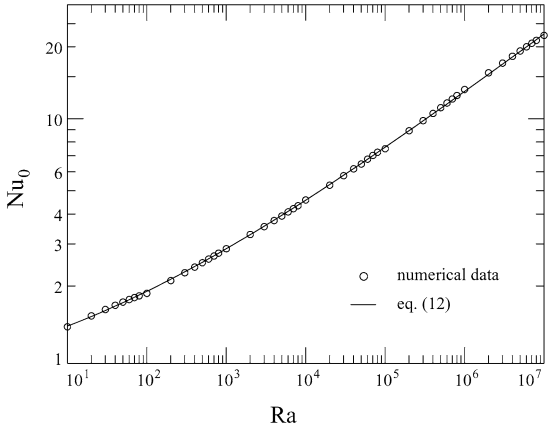

Fig. 6. Distribution of Nu_0 vs. Ra for the single cylinder.

so as to highlight in what measure the interactions of the bottom cylinder with the downstream top cylinder degrades its heat transfer performance relative to that of the single cylinder.

It may be seen that at a given cylinder-spacing S'/d, the heat transfer performance of the bottom cylinder starts being affected by the presence of the top cylinder, i.e., starts degrading, with a degree of degradation which increases as both S/d and Ra decrease, and as D/d increases.

In fact, at close cylinder-spacing the buoyant flow cannot penetrate completely the narrow space between the bottom and top cylinders, the smaller is the spacing, the weaker is the penetration strength, and thus the wider is the rear stagnation region of the bottom cylinder. In addition, the strength of the fluid motion around the cylinder, and thus the penetration strength, decreases with decreasing the Rayleigh number. Finally, as the diameter ratio increases, the separation angle of the fluid flow along the bottom cylinder surface decreases, which again implies an increase in the extent of the rear stagnation region of the bottom cylinder.

As regards the cylinder-spacing S'/d, which could be called *first critical cylinder-spacing* and calculated as the inter-cylinder spacing at which the ratio Nu_b/Nu_0 becomes equal to 1 ± 0.01, the distributions of S'/d vs. Ra for several values of D/d are reported in Fig. 4. As expected on account of the considerations stated above, S'/d increases as Ra decreases, and as D/d increases. In contrast, S'/d is practically independent of the temperature condition imposed at the top cylinder surface, which means that the bottom cylinder starts being affected by the presence of the top cylinder simply by the mechanical point of view.

Moreover, it seems worth noticing that at a *second critical cylinder-spacing* S''/d smaller than S'/d, the degree of degradation of the heat transfer performance of the bottom cylinder starts depending also on the temperature condition imposed at the top cylinder surface. Actually, for inter-cylinder spacings below S''/d, a larger amount of heat is exchanged at the bottom cylinder surface if the top cylinder surface is adiabatic rather than heated, as, e.g., clearly shown in Fig. 2 for $Ra = 10^3$. In fact, at very close spacing the heated top cylinder affects the heat transfer performance of the underneath cylinder not only by the mechanical point of view, but also by the thermal point of view, which implies a further decrease in the strength of the buoyancy-induced flow. The distributions of S''/d vs. Ra for several values of D/d are reported in Fig. 5. Like the first critical cylinder-spacing, also S''/d increases as Ra decreases, and as D/d increases.

6.2. Dimensionless correlating-equations

6.2.1. Single cylinder ($D/d = 0$)

The numerical results obtained for the average Nusselt number Nu_0 of the single cylinder may be expressed as a function of the Rayleigh number by the following semi-empirical binomial algebraic relation of the Churchill–Chu type:

$$Nu_0 = 0.701 + 0.411Ra^{0.25} \tag{12}$$

for $10^1 \leqslant Ra \leqslant 10^7$, with percent standard deviation of error $E_{sd} = 0.8\%$, and range of error E from -1.7% to $+2.1\%$, as shown in Fig. 6.

6.2.2. Bottom cylinder of a pair ($D/d > 0$) with top cylinder heated

The numerical results obtained for the average Nusselt number Nu_b of the bottom cylinder when the top cylinder surface

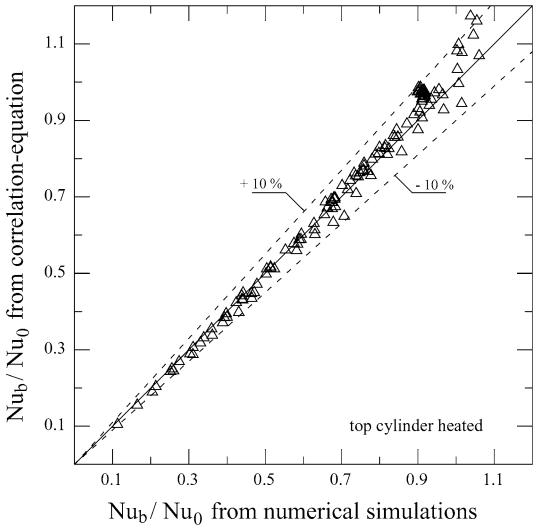

Fig. 7. Comparison between correlating equation and numerical results for the ratio Nu_b/Nu_0 with heated top cylinder.

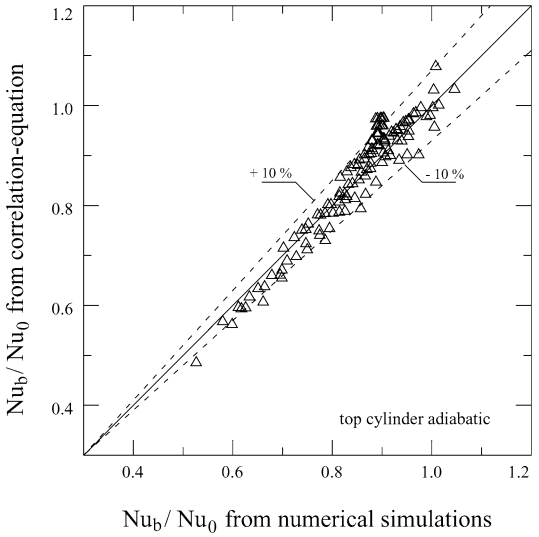

Fig. 8. Comparison between correlating equation and numerical results for the ratio Nu_b/Nu_0 with adiabatic top cylinder.

is heated at same temperature are expressed in terms of heat transfer effectiveness through the ratio Nu_b/Nu_0, which may be correlated to the independent dimensionless parameters Ra, S/d, and D/d, by the following semi-empirical transcendental equation:

$$\frac{Nu_b}{Nu_0} = a(S/d)^b \tag{13}$$

with

$$a = c\,Ra^d \tag{14}$$

$$b = e\,Ra^f \tag{15}$$

$$c = -0.219 \cdot \mathrm{Log}\left(\frac{D}{d}\right) + 0.838 \tag{16}$$

$$d = 0.031 \cdot \mathrm{Log}\left(\frac{D}{d}\right) + 0.019 \tag{17}$$

$$e = 0.187 \cdot \mathrm{Log}\left(\frac{D}{d}\right) + 0.133 \tag{18}$$

$$f = 0.041 \cdot \mathrm{Log}\left(\frac{D}{d}\right) + 0.056 \tag{19}$$

for $10^1 \leqslant Ra \leqslant 10^7$, $0.2 \leqslant S/d \leqslant 10$, and $0.2 \leqslant D/d \leqslant 25$, with percent standard deviation of error $E_{\mathrm{sd}} = 4.98\%$, and 94.7% of data within the range of error $E = \pm 10\%$, as shown in Fig. 7.

6.2.3. Bottom cylinder of a pair ($D/d > 0$) with top cylinder adiabatic

The numerical results obtained for the average Nusselt number Nu_b of the bottom cylinder when the top cylinder surface is adiabatic are expressed in terms of heat transfer effectiveness through the ratio Nu_b/Nu_0, which again may be correlated to the independent dimensionless parameters Ra, S/d, and D/d, through Eqs. (13)–(15) once the coefficients c, d, e, and f, are expressed by the following equations:

$$c = -0.192 \cdot \mathrm{Log}\left(\frac{D}{d}\right) + 0.871 \tag{20}$$

$$d = 0.031 \cdot \mathrm{Log}\left(\frac{D}{d}\right) + 0.015 \tag{21}$$

$$e = 0.039 \cdot \mathrm{Log}\left(\frac{D}{d}\right) + 0.028 \tag{22}$$

$$f = 0.078 \cdot \mathrm{Log}\left(\frac{D}{d}\right) + 0.056 \tag{23}$$

for $10^1 \leqslant Ra \leqslant 10^7$, $0.2 \leqslant S/d \leqslant 10$, and $0.2 \leqslant D/d \leqslant 25$, with percent standard deviation of error $E_{\mathrm{sd}} = 5.16\%$, and 94.0% of data within the range of error $E = \pm 10\%$, as shown in Fig. 8.

6.2.4. First critical cylinder-spacing

The numerical results obtained for the first critical cylinder-spacing S'/d may be correlated to the Rayleigh number Ra, and to the diameter ratio D/d, by the following semi-empirical equation:

$$\frac{S'}{d} = 4.98\left(\frac{D}{d}\right)^{0.256} Ra^B \tag{24}$$

with

$$B = -0.2\left(\frac{D}{d}\right)^{0.051} \tag{25}$$

for $10^1 \leqslant Ra \leqslant 10^7$, and $0.2 \leqslant D/d \leqslant 125$, with percent standard deviation of error $E_{\mathrm{sd}} = 8.04\%$, and range of error E from -10.8% to $+17.8\%$, as shown in Fig. 9.

6.2.5. Second critical cylinder-spacing

The numerical results obtained for the second critical cylinder-spacing S''/d may be correlated to the Rayleigh number Ra, and to the diameter ratio D/d, by the following semi-empirical equation:

$$\frac{S''}{d} = 2.52\left(\frac{D}{d}\right)^{0.262} Ra^B \tag{26}$$

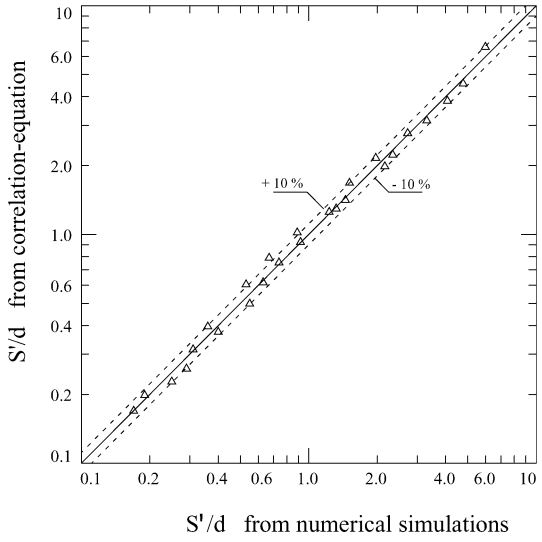

Fig. 9. Comparison between Eq. (24) and numerical results.

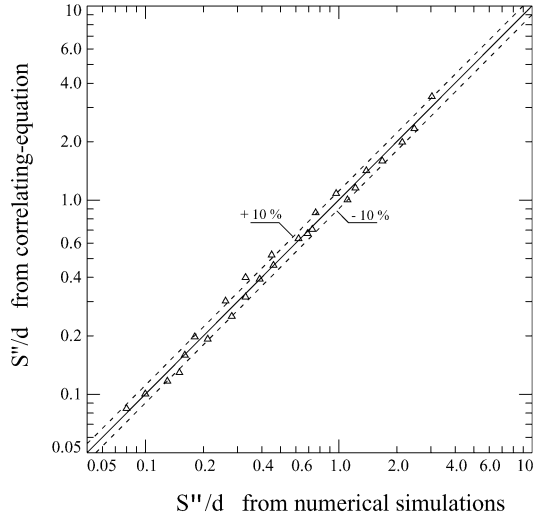

Fig. 10. Comparison between Eq. (26) and numerical results.

with

$$B = -0.2\left(\frac{D}{d}\right)^{0.051} \tag{27}$$

for $10^1 \leqslant Ra \leqslant 10^7$, and $0.2 \leqslant D/d \leqslant 125$, with percent standard deviation of error $E_{sd} = 9.35\%$, and range of error E from -13.9% to $+21.0\%$, as shown in Fig. 10.

7. Conclusions

Steady laminar free convection in air from an isothermal horizontal cylinder affected by a superimposed parallel cylinder of different diameter either at same temperature of the underneath cylinder or adiabatic, has been studied numerically through a computer-code based on the SIMPLE-C algorithm.

Simulations have been performed for ratios between the diameters of the upper and lower cylinders from 0 to 125, for inter-cylinder spacings from 0.1 up to more than 20 diameters of the bottom cylinder, and for values of the Rayleigh number based on the diameter of the bottom cylinder in the range between 10^1 and 10^7.

The main results obtained in the present study may be summarized as follows:

(a) the heat transfer performance of the bottom cylinder starts being affected by the presence of the top cylinder at a first critical cylinder-spacing S'/d which increases as Ra decreases, and as D/d increases, showing to be practically independent of the temperature condition imposed at the top cylinder surface;
(b) for cylinder-spacings smaller than the first critical cylinder-spacing, the degree of degradation of the heat transfer performance of the bottom cylinder increases as both S/d and Ra decrease, and as D/d increases;
(c) the degree of degradation of the heat transfer performance of the bottom cylinder starts depending also on the thermal condition imposed at the top cylinder surface at a second critical cylinder-spacing S''/d (smaller than S'/d), which increases as Ra decreases, and as D/d increases.

Finally, dimensionless correlating-equations have been developed for the heat transfer performance of the bottom cylinder, as well as for the first and the second critical cylinder-spacings.

References

[1] T. Chiang, J. Kaye, On laminar free convection from a horizontal cylinder, in: Proc. Fourth National Congress of Applied Mechanics, 1962, pp. 1213–1219.
[2] G. Wilks, External natural convection about two-dimensional bodies with constant heat flux, Int. J. Heat Mass Transfer 15 (1972) 351–354.
[3] S.W. Churchill, Laminar free convection from a horizontal cylinder with a uniform heat flux density, Lett. Heat Mass Transfer 1 (1974) 109–112.
[4] V.T. Morgan, The overall convective heat transfer from smooth circular cylinders, Adv. Heat Transfer 11 (1975) 199–264.
[5] J.H. Merkin, Free convection boundary layers on cylinders of elliptic cross section, J. Heat Transfer 99 (1977) 453–457.
[6] R.M. Fand, E.W. Morris, M. Lum, Natural convection heat transfer from horizontal cylinders to air, water and silicone oils for Rayleigh numbers between 3×10^2 and 2×10^7, Int. J. Heat Mass Transfer 20 (1977) 1173–1184.
[7] T.H. Kuehn, R.J. Goldstein, Numerical solution to the Navier–Stokes equations for laminar natural convection about a horizontal isothermal circular cylinder, Int. J. Heat Mass Transfer 23 (1980) 971–979.
[8] B. Farouk, S.I. Guceri, Natural convection from a horizontal cylinder—laminar regime, J. Heat Transfer 103 (1981) 522–527.
[9] B. Farouk, S.I. Guceri, Natural convection from a horizontal cylinder—turbulent regime, J. Heat Transfer 104 (1982) 228–235.
[10] Z.H. Qureshi, R. Ahmad, Natural convection from a uniform heat flux horizontal cylinder at moderate Rayleigh numbers, Numer. Heat Transfer 11 (1987) 199–212.
[11] P. Wang, R. Kahawita, T.H. Nguyen, Numerical computation of the natural convection flow about a horizontal cylinder using splines, Numer. Heat Transfer 17 (1990) 191–215.
[12] T. Saitoh, T. Sajiki, K. Maruhara, Bench mark solutions to natural convection heat transfer problem around a horizontal circular cylinder, Int. J. Heat Mass Transfer 36 (1993) 1251–1259.
[13] S.B. Clemes, K.G.T. Hollands, A.P. Brunger, Natural convection heat transfer from long horizontal isothermal cylinders, J. Heat Transfer 116 (1994) 96–104.

[14] K. Kitamura, F. Kami-iwa, T. Misumi, Heat transfer and fluid flow of natural convection around large horizontal cylinders, Int. J. Heat Mass Transfer 42 (1999) 4093–4106.
[15] G.F. Marsters, Natural convection heat transfer from a horizontal cylinder in the presence of nearby walls, Canad. J. Chem. Engrg. 35 (1975) 144–149.
[16] B. Farouk, S.I. Guceri, Natural and mixed convection heat transfer around a horizontal cylinder within confining walls, Numer. Heat Transfer 35 (1982) 329–341.
[17] E. Sparrow, D. Pfeil, Enhancement of natural convection heat transfer from a horizontal cylinder due to vertical shrouding surfaces, J. Heat Transfer 106 (1984) 124–130.
[18] F. Karim, B. Farouk, I. Namer, Natural convection heat transfer from a horizontal cylinder between confining adiabatic walls, J. Heat Transfer 108 (1986) 291–298.
[19] M.S. Sadeghipour, S.H. Kazemzadeh, Transient natural convection from a horizontal cylinder confined between vertical walls: A finite element solution, Int. J. Numer. Methods Engrg. 34 (1992) 621–635.
[20] L. Ma, Z. Vander, N.F. Vander Koo, F.T.M. Nieustadt, Natural convection around a horizontal circular cylinder in infinite space and within confining plates: A finite element solution, Numer. Heat Transfer, Part A 25 (1994) 441–456.
[21] G. Cesini, M. Paroncini, G. Cortella, M. Manzan, Natural convection from a horizontal cylinder in a rectangular cavity, Int. J. Heat Mass Transfer 42 (1999) 1801–1811.
[22] M.S. Sadeghipour, Y.P. Razi, Natural convection from a confined horizontal cylinder: the optimum distance between the confining walls, Int. J. Heat Mass Transfer 44 (2001) 367–374.
[23] H. Koizumi, I. Hosokawa, Chaotic behavior and heat transfer performance of the natural convection around a hot horizontal cylinder affected by a flat ceiling, Int. J. Heat Mass Transfer 39 (1996) 1081–1091.
[24] M.A. Atmane, V.S.S. Chan, D.B. Murray, Natural convection around a horizontal heated cylinder: The effects of vertical confinement, Int. J. Heat Mass Transfer 46 (2003) 3661–3672.
[25] E.M. Sparrow, D.S. Boessneck, Effect of traverse misalignment on natural convection from a pair of parallel, vertically stacked, horizontal cylinders, J. Heat Transfer 105 (1983) 241–247.
[26] M. Sadegh Sadeghipour, M. Asheghi, Free convection heat transfer from arrays of vertically separated horizontal cylinders at low Rayleigh numbers, Int. J. Heat Mass Transfer 37 (1994) 103–109.
[27] R. Chouikh, A. Guizani, M. Maalej, A. Belghith, Numerical study of the laminar natural convection flow around an array of two horizontal isothermal cylinders, Int. Comm. Heat Mass Transfer 26 (1999) 329–338.
[28] R. Chouikh, A. Guizani, A. El Cafsi, M. Maalej, A. Belghith, Experimental study of the laminar natural convection flow around an array of heated horizontal cylinders, Renewable Energy 21 (2000) 65–78.
[29] M. Corcione, Correlating equations for free convection heat transfer from horizontal isothermal cylinders set in a vertical array, Int. J. Heat Mass Transfer 48 (2005) 3660–3673.
[30] I. Tokura, H. Saito, K. Kisinami, K. Muramoto, An experimental study of free convection heat transfer from a horizontal cylinder in a vertical array set in free space between parallel walls, J. Heat Transfer 105 (1983) 102–107.
[31] B.E. Launder, T.H. Massey, The numerical prediction of viscous flow and heat transfer in tube banks, J. Heat Transfer 100 (1978) 565–571.
[32] J.P. Van Doormaal, G.D. Raithby, Enhancements of the simple method for predicting incompressible fluid flows, Numer. Heat Transfer 11 (1984) 147–163.
[33] S.V. Patankar, D.B. Spalding, A calculation procedure for heat, mass and momentum transfer in three-dimensional parabolic flows, Int. J. Heat Mass Transfer 15 (1972) 1787–1797.
[34] B.P. Leonard, A stable and accurate convective modelling procedure based on quadratic upstream interpolation, Comput. Methods Appl. Mech. Engrg. 19 (1979) 59–78.
[35] S.V. Patankar, Numerical Heat Transfer and Fluid Flow, Hemisphere, Washington, DC, 1980.
[36] S.W. Churchill, H.H.S. Chu, Correlating equations for laminar and turbulent free convection from a horizontal cylinder, Int. J. Heat Mass Transfer 18 (1975) 1049–1053.
[37] G.D. Raithby, K.G.T. Hollands, Laminar and turbulent free convection from elliptic cylinders with a vertical plate and horizontal circular cylinder as special cases, J. Heat Transfer 98 (1976) 72–80.
[38] T.H. Kuehn, R.J. Goldstein, Correlating equations for natural convection heat transfer between horizontal circular cylinders, Int. J. Heat Mass Transfer 19 (1976) 1127–1134.
[39] E.M. Sparrow, J.E. Niethammer, Effect of vertical separation distance and cylinder-to-cylinder temperature imbalance on natural convection for a pair of horizontal cylinders, J. Heat Transfer 103 (1981) 638–644.